



Title	Dissipative and Autonomous Square-Wave Self-Oscillation of a Macroscopic Hybrid Self-Assembly under Continuous Light Irradiation
Author(s)	Ikegami, Tomonori; Kageyama, Yoshiyuki; Obara, Kazuma; Takeda, Sadamu
Citation	Angewandte Chemie International Edition, 55(29), 8239-8243 https://doi.org/10.1002/anie.201600218
Issue Date	2016-07-11
Doc URL	http://hdl.handle.net/2115/72714
Rights	This is the peer reviewed version of the following article: Dissipative and Autonomous Square-Wave Self-Oscillation of a Macroscopic Hybrid Self-Assembly under Continuous Light Irradiation, which has been published in final form at 10.1002/anie.201600218. This article may be used for non-commercial purposes in accordance with Wiley Terms and Conditions for Use of Self-Archived Versions.
Type	article (author version)
File Information	Angew. Chem. Int. Ed. 55-29_8239-8243.pdf



[Instructions for use](#)

Tomonori Ikegami, Yoshiyuki Kageyama,* Kazuma Obara, and Sadamu Takeda*
Angew. Chem. Int. Ed. **2016**, *55*(29), 8239–8243. (DOI: 10.1002/anie.201600218)

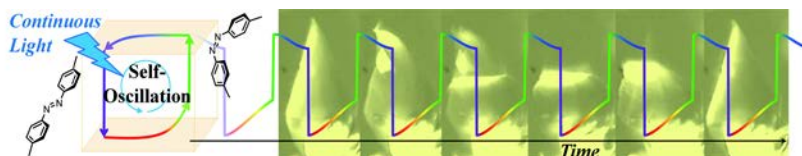
Dissipative and Autonomous Square-Wave Self-Oscillation of a Macroscopic Hybrid Self-Assembly under Continuous Light Irradiation

Tomonori Ikegami, Yoshiyuki Kageyama,* Kazuma Obara, and Sadamu Takeda*

Angewandte Chemie International Edition **2016**, *55*(29), 8239–8243. (DOI: 10.1002/anie.201600218)

Angewandte Chemie **2016**, *128*(29), 8379–8383. (DOI: 10.1002/ange.201600218)

COMMUNICATION



Self-organized supramolecular motor: A limit-cycle self-oscillatory motion of a macroscopic self-assembly was realized. The assembly permanently flips under continuous blue-light irradiation. Mechanical self-oscillation showing a spatio-temporal pattern is established by successively alternating photoisomerization processes and multistable phase transitions.

T. Ikegami, Y. Kageyama,* K. Obara,
S. Takeda*

Page 8239 – Page 8243

Dissipative and Autonomous Square-Wave Self-Oscillation of a Macroscopic Hybrid Self-Assembly under Continuous Light Irradiation

Dissipative and Autonomous Square-Wave Self-Oscillation of a Macroscopic Hybrid Self-Assembly under Continuous Light Irradiation

Tomonori Ikegami,^[c] Yoshiyuki Kageyama,^{*[a,b]} Kazuma Obara,^[a] and Sadamu Takeda^{*[a]}

Abstract: Building a bottom-up supramolecular system to perform continuously autonomous motions will pave the way for the next generation of biomimetic mechanical systems. In biological systems, hierarchical molecular synchronization underlies the generation of spatio-temporal patterns with dissipative structures. However, it remains difficult to build such self-organized working objects via artificial techniques. Here, we show the first example of a square-wave limit-cycle self-oscillatory motion of a noncovalent assembly of oleic acid and an azobenzene derivative. The assembly steadily flips under continuous blue-light irradiation. Mechanical self-oscillation is established by successively alternating photoisomerization processes and multistable phase transitions. These results offer a fundamental strategy for creating a supramolecular motor that works progressively under the operation of molecule-based machines.

There is considerable interest in macroscopically active materials and molecular robots generated by the incorporation of functional molecules.^[1–6] A key milestone in the mimicry of biological processes is the development of dissipative dynamics^[7] that show continuous and macroscopically patterned motions with dissipation of supplied energy via self-organization, but without the motion being trapped in a potential minimum.^[1] A typical phenomenon is self-oscillation, in which spatio-temporally patterned dynamics under the steady, but far-from-equilibrium, condition are generated by cooperative interactions within the system.^[1,8] To date, oscillatory working polymer gels have been realized by using the Belousov-Zhabotinsky reaction.^[9,10] We aim to develop autonomous, artificial, and supramolecular motions in an open system mimicking stimulus-responsive biological systems. For this reason, we prefer to construct the dissipative motions of macroscopic supermolecules triggered by small functional molecules, or so-called molecular machines.^[1,2]

Here, we show the first example of a macroscopic square-wave, self-oscillatory motion of a noncovalent assembly of oleic acid and an azobenzene derivative. The assembly flips repeatedly in an autonomous manner under continuous blue-light irradiation, as shown in Figure 1 and Movies S1–S3 in the supporting information (SI). Mechanical self-oscillation is established by successively alternating photoisomerization processes and multistable phase transitions.

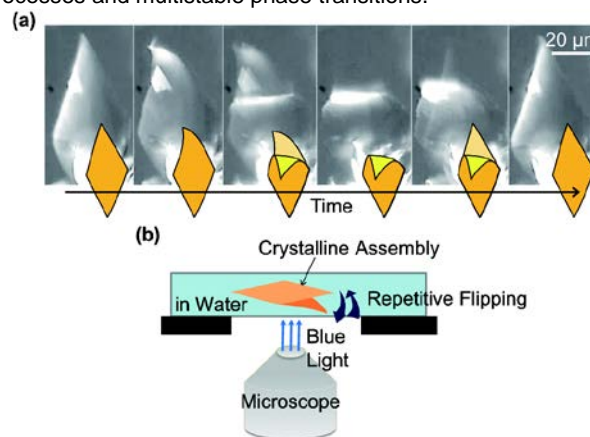


Figure 1. (a) Sequential micrographs (40x objective lens, bar is 20 μm) of one cycle of self-oscillation observed under 435-nm light, taken from Movie S1 in SI, and their schematic illustrations. (b) Schematic illustration showing setup for the observation of blue light-induced self-oscillation.

Azobenzenes have frequently been employed in the creation of photomechanically working objects^[3–5,11] and patterned dynamics.^[12,13] Azobenzene is isomerized from the *trans* to *cis* form by ultraviolet (UV) irradiation. Reverse isomerization is achieved through a thermal process or blue-light irradiation. This photoisomerization alters the volume of azobenzene and the orientation of the transition dipole moment. Repeatable macroscopic dynamics of azobenzene-containing materials have been realized by altering the wavelength of applied light or by coupling photo and thermal processes.^[3–5]

On the other hand, because blue light can induce *trans*-to-*cis* isomerization, repeated *trans*-to-*cis* and *cis*-to-*trans* photoisomerization events occur stochastically under blue-light irradiation. This property has been applied to create continuous working objects under photostationary-state (PSS) conditions. Credi demonstrated the repetitive unidirectional transit of a macrocycle of azobenzene-pseudorotaxane in solution under the PSS condition, in the absence of macroscopically synchronized transient dynamics.^[14] In contrast to an isotropic

[a] Dr. Y. Kageyama, K. Obara and Prof. S. Takeda
Department of Chemistry, Faculty of Science, Hokkaido University
Sapporo, 060-0810, Japan
E-mail: y.kageyama@mail.sci.hokudai.ac.jp,
stakeda@sci.hokudai.ac.jp

[b] Dr. Y. Kageyama
JST PRESTO
Kawaguchi, 332-0012, Japan

[c] T. Ikegami
Graduate School of Chemical Sciences and Engineering, Hokkaido University
Sapporo, 060-0810, Japan

Supporting information for this article is given via a link at the end of the document.

solution, repeated photoisomerization under polarized blue light results in a molecular ordering of azobenzene in condensed materials. Two-dimensional patterns have been formed on azobenzene-containing substrate surfaces^[12] or amphiphilic azobenzene monolayer membranes.^[13] Photo-driven oscillatory flipping of an azobenzene-polymer film could be produced by adjusting the direction of the incident polarized blue light, such that two sides of a film receive incident light alternatively owing to its flipping motion.^[11] Here, employing an entirely novel strategy, we achieved periodic flipping motions of azobenzene-containing noncovalent self-assemblies presented in aqueous dispersion in a dissipative and autonomous manner under continuous irradiation of nonpolarized blue light.

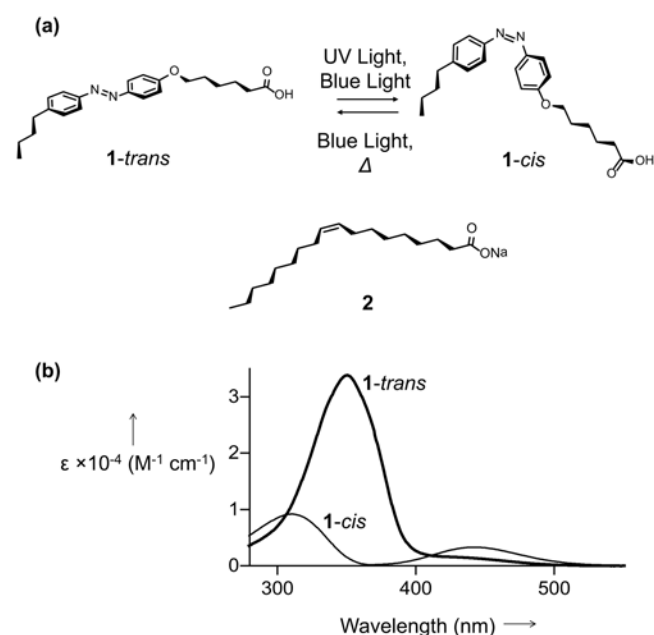


Figure 2. (a) Schematic illustration of the molecular structures of **1** and **2**, and the photoisomerization reaction of **1**. (b) UV-Vis absorption spectra of **1-trans** and **1-cis** in methanol. The absorption coefficient (ϵ) of **1-cis** was calculated from UV-Vis absorption spectra of a mixed solution of **1-trans** and **1-cis**, and from HPLC analysis of the mixed solution.

Table 1. Photochemical properties of **1** in methanolic solution.

Wavelength	$\epsilon_{trans} / \text{M}^{-1} \text{ cm}^{-1}$	$\epsilon_{cis} / \text{M}^{-1} \text{ cm}^{-1}$ [a]	<i>trans-cis</i> ratio in PSS ^[b]
435 nm	1.44×10^3	2.8×10^3	72 : 28
455 nm	1.10×10^3	2.7×10^3	76 : 24 [c]
470 nm	0.75×10^3	2.0×10^3	78 : 22

[a] Values calculated from UV-Vis absorption spectra of a mixed solution of **1-trans** and **1-cis**, and from HPLC analysis of the mixed solution. [b] Values obtained from HPLC analysis of a 0.372-mM methanolic solution of **1** under PSS. Quantum yields of *trans-to-cis* and *cis-to-trans* at 435 nm were 0.48 ± 0.02 and 0.59 ± 0.03 , respectively, with the same values being obtained at 470 nm. Experimental details are described in SI. [c] Using a handheld LED lamp as a light source, the ratio was 75:25, as shown in Figure 4d.

A mixed dispersion of an amphiphilic azobenzene (6-[4-(4-*n*-butylphenylazo)phenoxy]hexanoic acid, **1**) and sodium oleate (**2**) in a 4:6 molar ratio in phosphate-buffered solution (pH 7.5, 75 mM) was refrigerated (4 °C) for several days and allowed to form thin crystalline assemblies (Figure 2a). UV-Vis absorption spectra and photoisomerization properties of the *trans*- and *cis*-isomers of **1** in methanol are shown in Figure 2b and Table 1. An in-situ small-angle X-ray diffraction (SAXRD) experiment indicated that the *d*-spacing of the assemblies in the aqueous dispersion was 4.6 nm ($q = 1.37 \text{ nm}^{-1}$) (Figure 3a).^[15] Based on data from high-performance liquid chromatography (HPLC) analysis with UV-Vis and evaporative light scattering (ELS) detectors (Figure 4a), we determined that the assembly is in a 6:4 molar ratio of **1** to **2**. The *d*-spacing value and composition ratio remained constant when the preparation was made with a 2:8 or 1:9 molar ratio mixture of **1** and **2**, indicating that the assembly was stoichiometrically uniform.^[16] Fourier transform infrared (FTIR) microspectrometry yielded a strong peak at 1706 cm^{-1} , which we assigned to the stretching mode of the hydrogen-bonded carboxyl groups (Figure S1 in SI). These results suggest that this crystalline assembly has a lamellar structure, in sharp contrast to our previously obtained photo-driven soft liquid crystals composed of **1** and **2**.^[5,17] Using a differential interference contrast (DIC) microscope equipped with a high-pressure mercury lamp in its fluorescent unit, we found an oscillatory bending-unbending motion of the crystalline assembly of around 1 μm in thickness under nonpolarized 435-nm light irradiation (Figure 1, and Movie S1 in SI). The frequency of the motion increased with increasing light intensity. A similar oscillation was observed under 470-nm light irradiation, but the assembly collapsed under 365-nm light irradiation.^[18]

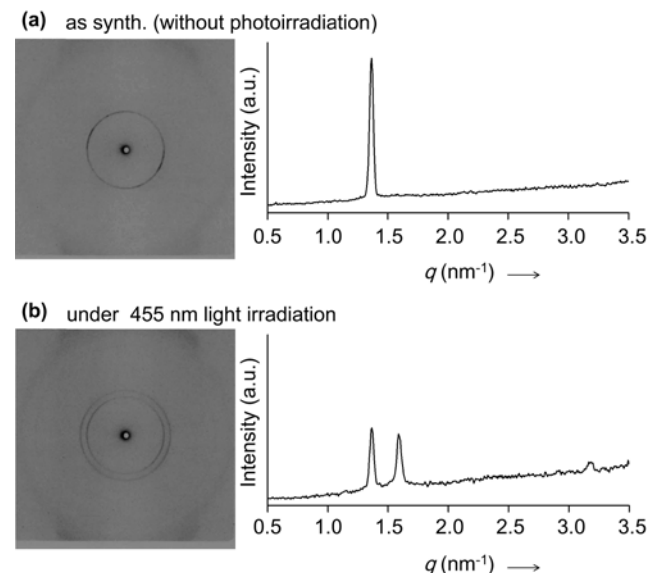


Figure 3. In-situ SAXRD fringe images and profiles of assemblies measured (a) under the dark condition, and (b) under continuous 455-nm light irradiation.

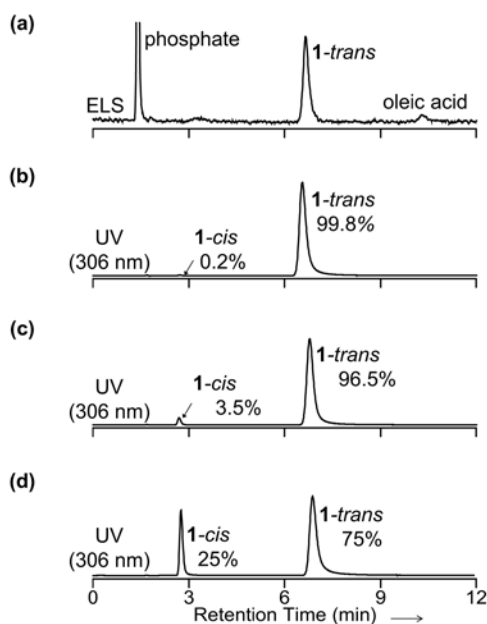


Figure 4. Results of HPLC analyses. Chromatographs of assemblies as synthesized under the dark condition, recorded using the (a) ELS detector and (b) UV detector (monitored at 306 nm, an isosbestic point of **1-trans** and **1-cis**). (c) Chromatograph of assemblies after 455-nm light irradiation. (d) Chromatograph of a methanolic solution of **1** after 455-nm light irradiation.

Figure 5a shows the time profile of oscillation for our plate-like crystalline assembly captured by a high-speed camera (1000 fps) under 435-nm light irradiation (Movie S2 in SI). The oscillation cycle consisted of four steps: sluggish bending of the flat assembly (S1), rapid morphological change of the assembly to a bent form (S2), sluggish unbending of the assembly (S3), and rapid return to the original morphology (S4). The time span of each step S_n is presented in the form τ_n . The displacement magnitude for each step remained constant with changes in the power of incident light. The oscillatory frequency and values of $1/\tau_1$ and $1/\tau_3$ increased with increasing light intensity, whereas each value of τ_2 and τ_4 for the assembly remained constant at 3 ± 1 ms (Figure S3 in SI).

Self-oscillatory motion was generally observed in thin plate-like crystals of various shapes under continuous 435-nm light irradiation in a four-step manner^[19] (Figure 5b). The magnitude of displacement and time (τ) for each step differed from those of the assembly in Figure 5a. However, similarly to the time profile in Figure 5a, both $1/\tau_1$ and $1/\tau_3$ were proportional to the applied light intensity (slopes in Figure 5d are 1), whereas τ_2 and τ_4 remained constant when the irradiation intensity was changed. These results indicate that S1 and S3 are one-photon processes. In contrast, the motions of S2 and S4 are not directly induced by individual photons, but by the intrinsic structures of the assemblies.

The in-situ SAXRD profile of crystalline assemblies in aqueous dispersion was measured under 455-nm light irradiation with a handheld LED lamp (λ span = 445–485 nm) (Figure 3b). Because the exposure time (60 min) far exceeded the oscillation cycle period, the structures of the S1 and S3 states could both be detected. Two peaks appeared, one of which was assigned to the original crystalline phase ($d = 4.6$ nm). The other peak ($d = 4.0$ nm, $q = 1.59$ nm⁻¹), which developed *de*

novo under blue-light irradiation, represented the other polymorphic phase of a bistable crystal under irradiation. This crystalline sample showed self-oscillatory motion under 435-nm light irradiation, both before and after the SAXRD measurement.

The HPLC experiment revealed that the percentages of **1-trans** and **1-cis** in the synthesized crystalline assembly were 99.8% and 0.2%, respectively, in the dark (Figure 4b). In a methanolic solution, the steady-state ratio of **1-trans** to **1-cis** under continuous 455-nm light irradiation with the handheld LED was 75:25 (Figure 4d). Under the same light-irradiation condition, the ratio in the crystalline assemblies was 96.5:3.5, which is the average ratio of **1-trans** and **1-cis** while the crystals are oscillating (Figure 4c). One reason for the difference in ratios between the methanolic solution and crystalline assemblies is that the regular packing of molecules in the crystal inhibits *cis*-isomer formation (as discussed in depth elsewhere).^[20] The strength of the inhibition differs across two distinguishable polymorphic phases, owing to the difference in the molecular packing of the phase.

In methanolic solution, ratios of the absorption coefficients of **1-trans** to **1-cis** were larger at 435 nm than at 470 nm, whereas the quantum yields of photoisomerization were equivalent (see Table 1). Assuming that the relationships of **1** and **2** remain as they are in the crystalline phase, the kinetic ratio of the *trans*-to-*cis* to *cis*-to-*trans* isomerization should be larger under 435- than under 470-nm light. Figure 5c shows the time profile of the same assembly as shown in Figure 5b, but under 470-nm light irradiation.^[21] The increased τ_1 to τ_3 ratio under 470-nm light irradiation indicates that there is a net *trans*-to-*cis* isomerization in S1 and, conversely, a net *cis*-to-*trans* isomerization in S3. This switching process is discussed in detail in SI.

The self-oscillation dynamics can be summarized as follows (Figure 5e). In S1, the photoreaction increases the population of *cis*-isomer. However, due to instability of the original phase with increased *cis*-isomer levels, the morphology of the crystalline assembly changes in S2. Subsequently, the photoreaction decreases the population of *cis*-isomer in S3. This decrease likely is due to a change in the photoisomerization quantum yield, owing to the molecular arrangement in the new polymorphic phase. Alternatively, the *cis*-isomer decrease might be due to an increase in the absorption cross-section ratio of *cis*- compared to *trans*-isomer in the new polymorphic phase. When the *trans*-isomer fraction reaches a threshold, the assembly returns to its original morphology because of the stability of the original crystalline phase, which is characterized by a small portion of *cis*-isomer, in S4. By repeating this cycle, the crystalline assembly shows square-wave periodic self-oscillation with a constant amplitude and light intensity-dependent frequency.

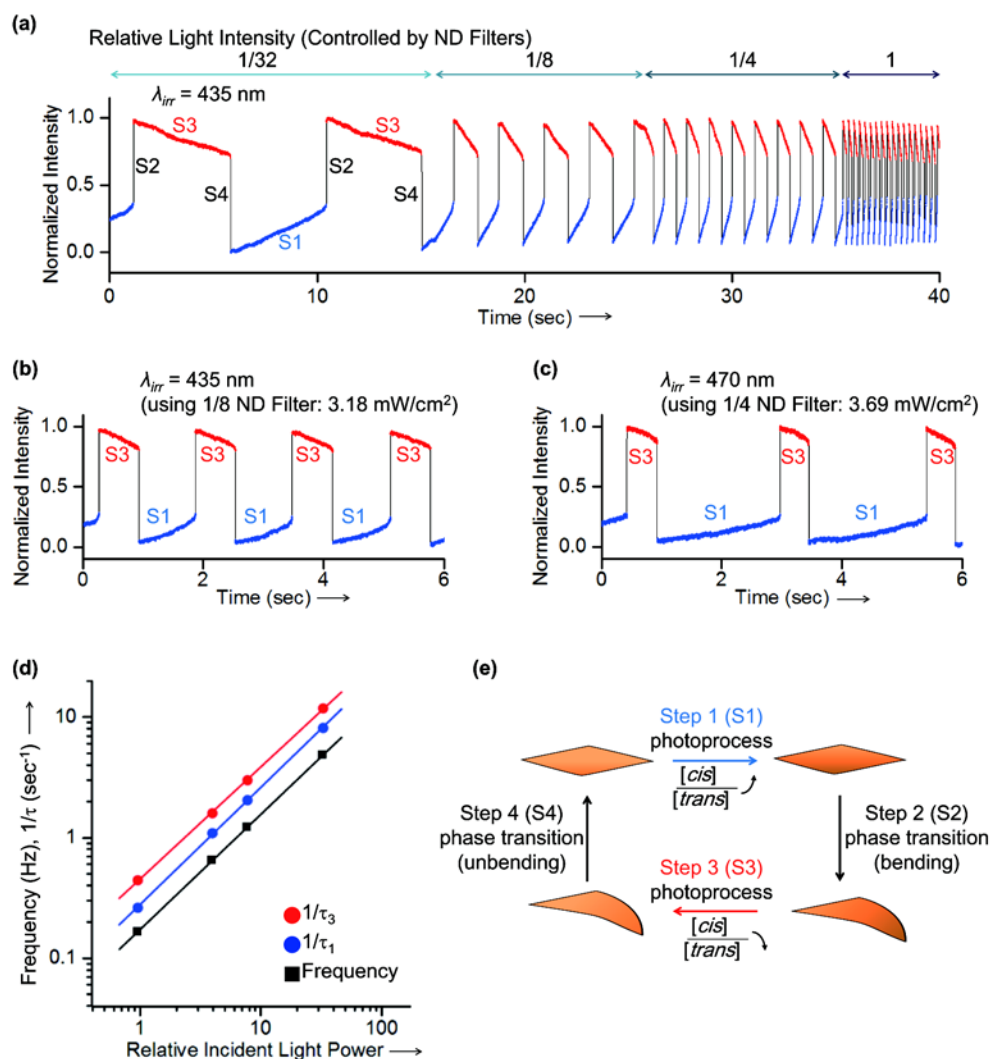


Figure 5. Time profiles of self-oscillations. Each intensity on the vertical axis was determined from the brightness change of a region of the assembly recorded by the microscope (20 \times objective lens) and normalized using the two extreme values. **(a)** Time profile of self-oscillation of a crystalline assembly under various intensities of incident light (Movie S2 in SI). **(b, c)** Time profiles of self-oscillations of another crystalline assembly under **(b)** 435-nm light and **(c)** 470-nm light. **(d)** Frequency and time spans of S1 and S3 as a function of intensity of 435-nm light for the crystalline assembly in **(b)**. Slopes indicate that S1 and S3 are one-photon processes. **(e)** Schematic illustration of each step of the self-oscillatory motion.

The macroscopic self-oscillation reported here is a type of autonomous limit-cycle oscillation that shows repeated flips in a steady manner under continuous photoirradiation. Oscillation parameters, such as amplitude and frequency, depend on the properties (e.g., thickness) of individual assemblies (Movie S3 in SI). Previously reported photo-driven oscillators have been intrinsically limited in their flipping direction by the orientation and polarization of the external light source.^[11] By contrast, the self-oscillation presented here is realized by an autonomous combination of a change of photoisomerization efficiency and phase transitions of the molecular assembly. This bistable

switching mechanism may be widely and universally applicable for producing macroscopic molecular motors that function in temporally multimodal frequencies with spatially organized motions by arranging the shapes and components of the assemblies. As shown in Movie S4 in SI, a frog-kick motion of a waving ribbon composed of **1**, **2**, and stearic acid was realized.^[22] Moreover, because the bistability switching reaction is not limited to photoisomerization, this mechanism has potential utility for the creation of autonomous motors triggered by a wide range of chemical machines. The importance of this study lies in the realization of macroscopic self-oscillation by the repeated reversible reaction of a molecular machine with the cooperative transformation of a molecular assembly. These results provide a fundamental strategy for constructing dynamic self-organizations in supramolecular systems to achieve bioinspired molecular systems.^[1,23]

Experimental Section

Materials

Sodium oleate (extra-pure grade, **2**) was purchased from Junsei Chemical and used without further purification. The azobenzene derivative (6-[4-(4-*n*-butylphenylazo)phenoxy]hexanoic acid, **1**) was used after synthesis by a method described previously.^[5]

General method for preparation of the crystalline self-assembly

A mixed solution of CH₂Cl₂ and MeOH (1:1 volume ratio) containing **1** and **2** (4:6 molar ratio) was dispensed in a glass vial. Solvent was evaporated in vacuo to obtain an amorphous mixture of **1** (0.64 mg, 1.7 μmol) and **2** (0.80 mg, 2.6 μmol). To the amorphous mixture was added 0.25 mL of an aqueous solution of NaOH (1.7 μmol), followed by 0.25 mL of phosphate buffered water (pH 7.5, 150 mM). Substrates were ultrasonicated for 30 min to obtain a pale yellow dispersion. The dispersion was placed on a glass slide, sealed with a frame-seal (17 × 28 mm) incubation chamber (Bio-Rad), and refrigerated (4 °C) for 3 days. Motion was then observed under a microscope. For spectrometric, HPLC, and SAXRD analyses, a crystalline assembly sample was prepared from the dispersion, as described in detail below.

Observation and analysis of macroscopic motion under light irradiation

For microscopic observation, a DIC microscope (Nikon, TE2000) was used, which was equipped with a mercury lamp epi-fluorescence unit and filter units (UV-1A for 365-nm, BV-1A for 435-nm, and B-2A for 470-nm irradiation). The bandwidths of the filter units were 10 nm for UV-1A and BV-1A, and 40 nm for B-2A. Objective lenses of Nikon Plan Fluor ELWD 20× (NA 0.45) and Nikon Plan Fluor ELWD 40× (NA 0.60) were used. To reduce the incident light intensity, 1/4 and 1/8 neutral density (ND) filters were attached to the TE2000 system. Powers of the 435-nm light when using a 20× objective lens with no ND filters, the 1/4 ND filter, the 1/8 ND filter, and both filters were measured as 26.4, 6.25, 3.18, and 0.76 mW/cm², respectively, by a power meter (Sanwa, LP1 Mobiken). Powers obtained with 470-nm light were 0.59 times smaller than those with 435-nm light. One charge-coupled device camera (Sentech STC-TC152USB) was used to take movies, and another (Ditect, HAS-220) was used to obtain high-speed sequential images. To analyze the motion, the Image-Pro Premier software (Media Cybernetics) was used.

In-situ SAXRD measurement

After the supernatant of the dispersion was removed, the concentrated dispersion was placed into a glass capillary (1-mm diameter, Hilgenberg GmbH), which was placed in the SAXRD apparatus (Rigaku, Nanoviewer IP). Fringes were recorded for 60 min of exposure. To record the fringes under blue-light irradiation, light from a handheld LED lamp (Optcode, LED-455P) was focused on the sample by using a lens. The bandwidth of the lamp is about 35 nm.

HPLC for composition analysis of the assembly

All experiments were carried out under a red lamp in a dark room by using an HPLC system (JASCO, LC2000) that was equipped with an octadecylsilane column (Nacalai Tesque, Cosmosil 5C₁₈-AR-II), UV detector (JASCO, UV2075), and ELS detector (Agilent, 1260ELSD). The eluent was a 9:1 mixed solution of methanol and 0.05% (v/v) TFA aqueous solution.

The supernatant of the dispersion was removed completely, and crystalline self-assemblies were dissolved in methanol. Then, 5 μL of the solution were loaded into the HPLC instrument. To quantify the concentration of **1**, absorption of λ = 306 nm light (an isosbestic point of *trans*- and *cis*-isomers of **1**) was recorded. To quantify the concentration of **2**, the ELS detector was used, with the nebulizer and evaporator at

40 °C and the N₂ flow rate at 1.60 standard liters per minute. To determine the ratio of **1** and **2**, a calibration curve method was used.

To measure the photoisomerization yield in the crystalline self-assembly after light irradiation, separate assemblies were irradiated by the 455-nm LED lamp for 1 min, dissolved in methanol, and loaded on the same apparatus. To determine the ratio of *trans*- and *cis*-isomers, the ratio of the absorption peak areas was used. The photoisomerization yield in methanolic solution shown in Figure 4d was similarly measured.

Measurement and calculation of photochemical properties of **1** in methanolic solution

All experiments were carried out in a dark room. Methanolic solutions of **1** (0.0294 and 0.744 mM) kept in the dark were analyzed by a UV-Vis spectrometer (JASCO V650) to determine the absorption spectrum of **1-trans**. A methanolic solution of **1** (0.372 mM) was irradiated by 435-, 455-, and 470-nm light with a 150-W Xe lamp in a spectrofluorometer (JASCO FP-8300, bandwidth = 5 nm) to prepare different ratios of *trans* and *cis* under each PSS. The same spectrometer was used to obtain the absorption spectra of the solutions. Ratios of *trans*- and *cis*-isomers were measured by HPLC (monitored at 412 nm, an isosbestic point of **1-trans** and **1-cis**). The molar absorption coefficient of **1-cis** was calculated from the measured absorption spectra and HPLC data.

Acknowledgements

This work was funded by JST PRESTO (Molecular Technology). The SAXRD experiment was carried out at the CRIS OPEN FACILITY (Hokkaido Univ.).

Keywords: Molecular devices • Nonequilibrium processes • Cooperative effects • Phase transitions • Photochromism

- [1] a) E. R. Kay, D. A. Leigh, *Angew. Chem. Int. Ed.* **2015**, *51*, 10080–10088; *Angew. Chem.* **2015**, *127*, 10218–10226; b) J.-M. Lehn, *Angew. Chem. Int. Ed.* **2015**, *54*, 3276–3289; *Angew. Chem.* **2015**, *127*, 3326–3340; c) E. Mattia, S. Otto, *Nat. Nanotech.* **2015**, *10*, 111–119; d) M. von Delius, D. A. Leigh, *Chem. Soc. Rev.* **2011**, *40*, 3656–3676; e) B. A. Grzybowski, C. E. Wilmer, J. Kim, K. P. Browne, K. J. M. Bishop, *Soft Matter* **2009**, *5*, 1110–1128; f) M. Orlik, *J. Solid State Electrochem.* **2009**, *13*, 245–261; g) E. R. Kay, D. A. Leigh, F. Zerbetto, *Angew. Chem. Int. Ed.* **2007**, *46*, 72–191; *Angew. Chem.* **2007**, *119*, 72–196; h) W. R. Browne, B. L. Feringa, *Nat. Nanotech.* **2006**, *1*, 25–35.
- [2] V. Balzani, A. Credi, M. Venturi, in *Molecular Devices and Machines – A Journey into the Nanoworld*, WILEY-VCH, Weinheim, **2003**.
- [3] a) P. Naumov, S. Chizhik, M. K. Panda, N. K. Nath, E. Boldyreva, *Chem. Rev.* **2015**, *115*, 12440–12490. b) T. Ube, T. Ikeda, *Angew. Chem. Int. Ed.* **2014**, *53*, 10290–10299; *Angew. Chem.* **2014**, *126*, 10456–10465. c) A. Priimagi, C. J. Barrett, A. Shishido, *J. Mater. Chem. C* **2014**, *2*, 7155–7162; d) T. Aida, E. W. Meijer, S. I. Stupp, *Science* **2012**, *335*, 813–817; e) A. Natansohn, P. Rochon, *Chem. Rev.* **2002**, *102*, 4139–4175.
- [4] a) S. Iamsaard, S. J. Aßhoff, B. Matt, T. Kudernac, J. J. L. M. Cornelissen, S. P. Fletcher, N. Katsonis, *Nature Chem.* **2014**, *6*, 229–235; b) M. Baroncini, C. Gao, V. Carboni, A. Credi, E. Previtera, M. Semeraro, M. Venturi, S. Silvi, *Chem. Eur. J.* **2014**, *20*, 10737–10744; c) L. Osorio-Planes, M. Espelt, M. A. Pericàs, P. Ballester, *Chem. Sci.* **2014**, *5*, 4260–4264.
- [5] Y. Kageyama, N. Tanigake, Y. Kurokome, S. Iwaki, S. Takeda, K. Suzuki, T. Sugawara, *Chem. Commun.* **2013**, *49*, 9386–9388.
- [6] a) R. Eelkema, M. M. Pollard, J. Vicario, N. Katsonis, B. S. Ramon, C. W. M. Bastiaansen, D. J. Broer, B. L. Feringa, *Nature* **2006**, *440*, 163; b) J. Berná, D. A. Leigh, M. Lubomska, S. M. Mendoza, E. M. Pérez, P. Rudolf, G. Teobaldi, F. Zerbetto, *Nat. Mater.* **2005**, *4*, 704–710; c) Y. Liu, A. H. Flood, P. A. Bonvallet, S. A. Vignon, B. H. Northrop, H.-R.

- Tseng, J. O. Jeppesen, T. J. Huang, B. Brough, M. Baller, S. Magonov, S. D. Solares, W. A. Goddard, C.-M. Ho, J. F. Stoddart, *J. Am. Chem. Soc.* **2005**, *127*, 9745–9759.
- [7] a) P. Glansdorff, I. Prigogine, *Physica*, **1964**, *30*, 351–374; b) G. Nocolis, I. Prigogine, in *Self-Organization in Nonequilibrium Systems: From Dissipative Structures to Order through Fluctuations* (Japanese Transl. Iwanami, **1980**), John Wiley & Sons, Inc., New York **1977**.
- [8] For examples, a) T. Rungsimanon, K. Yuyama, T. Sugiyama, H. Masuhara, *Cryst. Growth. Des.* **2010**, *10*, 4686–4688, b) H. Kitahata, K. Kawata, Y. Sumino, S. Nakata, *Chem. Phys. Lett.* **2008**, *457*, 254–258.
- [9] A. Zaijin, A. M. Zhabotinsky, *Nature* **1970**, *225*, 535–537.
- [10] a) R. Yoshida, *Self-oscillating polymer gels*, in *Supramolecular Soft Matter*, (Nakanishi, T. Eds.) John Wiley & Sons, New Jersey, **2011**, chap. 12. b) H. Zhou, Z. Zheng, Q. Wang, G. Xu, J. Li, X. Ding, *RSC Adv.* **2015**, *5*, 13555–13569;
- [11] a) S. Serak, N. Tabiryan, R. Vergara, T. J. White, R. A. Vaia, T. J. Bunning, *Soft Matter* **2010**, *6*, 779–783; b) T. J. White, N. V. Tabiryan, S. V. Serak, U. A. Hrozhyk, V. P. Tondiglia, H. Koerner, R. A. Vaia, T. J. Bunning, *Soft Matter* **2008**, *4*, 1796–1798.
- [12] X. L. Jiang, L. Li, J. Kumar, D. Y. Kim, V. Shivshankar, S. K. Tripathy, *App. Phys. Lett.* **1996**, *68*, 2618–2620.
- [13] Y. Tabe, H. Yokoyama, *Langmuir* **1995**, *11*, 4609–4613.
- [14] G. Ragazzon, M. Baroncini, S. Silvi, M. Venturi, A. Credi, *Nat. Nanotech.* **2015**, *10*, 70–75.
- [15] Wide-range XRD profile of the crystalline assembly is shown in Figure S2 in SI.
- [16] After drying, the hydrated crystalline assembly was transformed into the other phase under ambient atmosphere. Therefore, X-ray single-crystal analysis was not able to be carried out successfully.
- [17] The structure of the helical assembly of oleic acid was revealed to be an inverted hexagonal assembly. Details are reported in Y. Kageyama, T. Ikegami, N. Hiramatsu, S. Takeda, T. Sugawara, *Soft Matter* **2015**, *11*, 3550–3558.
- [18] Self-oscillatory motion was also observed under focused light from the 455-nm handheld LED lamp. Dehydrated crystalline assemblies did not show any motion under 435-, 455-, or 470-nm light irradiation.
- [19] Most of the thin plate-like crystals showed self-oscillation in a four-step manner. On the other hand, some crystals having large areas or complex structures showed multistep oscillation.
- [20] a) L. Xing, W. L. Mattice, *Langmuir* **1996**, *12*, 3024–3030; b) M. Matsumoto, S. Terretaz, H. Tachibana, *Adv. Colloid Interface Sci.* **2000**, *87*, 147–164.
- [21] Under 470-nm light, S1 and S3 were also one-photon processes, as shown in Figure S4 in SI.
- [22] Self-oscillatory motion was observed regularly in the thin-plate crystalline assemblies of **1** and **2**. Some crystalline assemblies composed of **1** and other fatty acids, such as stearic acid and palmitoleic acid, showed various self-oscillatory motions, such as waving, rowing, and blowing motions. In our study, no macroscopic oscillations were observed in crystals of **1** without fatty acids. Detailed studies of these processes are ongoing.
- [23] a) K. Ruiz-Mirazo, C. Briones, A. Escosura *Chem. Rev.* **2014**, *114*, 285–366. b) J. R. Nitschke, *Nature* **2009**, *462*, 736–738.